Biosensors and Bioelectronics 44 (2013) 64–69

Contents lists available at SciVerse ScienceDirect

Biosensors and Bioelectronics

journal homepage: www.elsevier.com/locate/bios

Construction of an amperometric bilirubin biosensor based on covalent immobilization of bilirubin oxidase onto zirconia coated silica nanoparticles/chitosan hybrid film

Bhawna Batra [a], Suman Lata [a], Sunny [b], J.S. Rana [b], Chandra Shekhar Pundir [a,*]

[a] Department of Biochemistry, M.D.University, Rohtak 124 001, Haryana, India
[b] Department of Biotechnology, D.C.R. University of Science and Technology, Murthal, Sonepat 131039, India

ARTICLE INFO

Article history:
Received 23 October 2012
Received in revised form
14 December 2012
Accepted 17 December 2012
Available online 16 January 2013

Keywords:
Bilirubin
Bilirubin oxidase
Bilirubin biosensor
Zirconia coated silica nanoparticles
Chitosan
Serum

ABSTRACT

A method is described for the construction of a highly sensitive electrochemical biosensor for the detection of bilirubin. The sensor is based on covalent immobilization of bilirubin oxidase (BOx) onto zirconia coated silica nanoparticles (SiO_2@ZrONPs)/chitosan (CHIT) composite electrodeposited onto Au electrode. The enzyme electrode was characterized by scanning electron microscopy (SEM), Fourier transform infra-red spectroscopy (FTIR), cyclic voltammetry (CV) and electrochemical impedance spectroscopy (EIS). The biosensor showed optimum response within 2 s at pH 8.5 (0.1 M Tris–HCl) and 35 °C, when operated at 20 mV s^{-1}. The biosensor exhibited excellent sensitivity (detection limit as 0.1 nM), fast response time and wider linear range (from 0.02 to 250 μM). Analytical recovery of added bilirubin was 95.56–97.0%. Within batch and between batch coefficients of variation were 3.2% and 3.35% respectively. The enzyme electrode was used 150 times over a period of 120 days, when stored at 4 °C. The biosensor measured bilirubin levels in sera of apparently healthy and persons suffering from jaundice, which correlated well with a standard colorimetric method (r=0.99).

1. Introduction

Bilirubin (formerly known as hematoidin) is a yellow colored breakdown product of normal heme catabolism. Heme is a principal component of hemoglobin, found in red blood cells. The normal levels of serum bilirubin are as follows—direct (also called conjugated) bilirubin: 0–0.3 mg/dL and total bilirubin: 0.3–1.9 mg/dL. Bilirubin is excreted in bile and urine, and its elevated levels in serum indicate jaundice, brain damage thalassemia, sphaerocytosis, Gilbert syndrome, heamolytic uremic syndrome and sickle cell anemia. It is responsible for yellow color of bruises, urine (via its reduced breakdown product, urobilin) discoloration in jaundice and brown color of feces (via its conversion to stercobilin). Bilirubin is generated by the action of biliverdin reductase on biliverdin, a green tetrapyrrolic bile pigment and also a product of heme catabolism. Bilirubin, when oxidized, reverts to biliverdin again. This cycle has led to the hypothesis that bilirubin's main physiologic role is as a cellular antioxidant (Baranano et al., 2002; Liu et al., 2008). Thus, determination of bilirubin in biological fluid is of great importance in the differential diagnosis of jaundice. Serum bilirubin levels are also clinically determined as part of the routine in newborn nurseries. This is because high concentrations of bilirubin in the blood may cause brain damage or even death, specifically in the case of babies (Maisels, 2009). Therefore, a cost effective measurement of bilirubin level is essential for the diagnosis and medical management of jaundice patients. Various methods have been reported for the measurement of bilirubin, the most common detection methods are the direct spectroscopic measurement (Doumas et al., 1973) and the diazo reaction (Bergmeyer et al., 1985). However, the direct spectroscopic measurement of bilirubin suffers from interference by other heme proteins, while the diazo reaction is pH dependent (Li and Rosenzweig, 1997). Other analytical methods for bilirubin determination such as polarography (Wang et al., 1985), and fluorometry (Koch and Oakingbe, 1981) require costly equipment, time consuming sample preparation and skilled persons to operate, and thus are not suitable for routine use. Nevertheless, biosensing methods are comparatively more simple, rapid and sensitive than these methods and require no sample pre-treatment. Electrochemical amperometric bilirubin biosensors employing bilirubin oxidase (BOx) are based on either the measurement of decreasing level of molecular oxygen (Wang and Ozsoz, 1990) or oxidation of hydrogen peroxide (Fortuney and Guilbault, 1996) or the mediated electron transfer by the Mn(II) ion using a conductive poly-terthiophene–Mn(II) complex (Rahmana et al., 2008). However these biosensors

* Corresponding author. Tel.: +91 9416492413; fax: +91 126274640.
E-mail address: pundircs@rediffmail.com (C.S. Pundir).

0956-5663/$ - see front matter © 2013 Elsevier B.V. All rights reserved.
http://dx.doi.org/10.1016/j.bios.2012.12.034

also have certain disadvantages such as low detection limit due to poor electron flow and lower storage stability of the enzyme electrode.

Recently, nanomaterials have been employed to improve the analytic performance of biosensors. Coated nanoparticles are essentially defined as the particles containing a core and a shell, having dimensions in the nanometer range. Composite nanoparticles exhibit improved physical and chemical properties over their single-component counterparts, and hence are potentially useful in a wide range of applications. These composite nanoparticles exhibit a variety of novel properties e.g., optical, electrical, catalytic, magnetic, and mechanical. Zirconia coated silica nanoparticles have been used as an efficient catalyst.

Chitosan (CHIT) is an important biopolymer for immobilization of biomolecules, due to its excellent film-forming ability, high permeability, mechanical strength, non-toxicity, biocompatibility, low cost and easy availability. Further, $-NH_2$ groups of CHIT provides hydrophilic environment for the biomolecules (Wang et al., 2010). We describe herein a novel approach of immobilizing bilirubin oxidase onto SiO_2@ZrONPs/CHIT modified Au electrode, its characterization and application for amperometric determination of bilirubin.

2. Experimental section

2.1. Materials

Bilirubin oxidase (BOx) from Sigma-Aldrich, St. Louis, USA, tetraethylorthosilicate (TEOS) from Fluka, Mumbai, India, and potassium chloride (KCl), bilirubin, chitosan and zirconium oxide nanoparticles (ZrONPs) from SISCO Research Laboratory, Mumbai, India were used. Double distilled water (DW) was used throughout the experimental studies.

2.2. Assay of free BOx

The assay of free BOx was carried out as described by Satyapal and Pundir (1993) with modifications. The assay was based on the quantification of H_2O_2, generated from oxidation of bilirubin catalyzed by BOx, using a color reaction consisting of the 4-aminophenazone, phenol and peroxidase as chromogenic system. The reaction mixture containing 0.7 ml of Tris–HCl buffer pH 8.5 (0.1 M), 0.1 ml of bilirubin solution (34.21 μM), and 0.1 ml of BOx solution (5 U/ml) was incubated at 37 °C for 10 min. Color reagent (1.0 ml) was added to the reaction mixture and kept at 37 °C in dark to develop the pink color. After 15 min, A_{520} was read and H_2O_2 concentration in the reaction mixture was interpolated from the standard curve between A_{520} vs. H_2O_2.

One unit of enzyme is defined as the amount of enzyme required to catalyze the formation of 1.0 μmol of H_2O_2 from oxidation of bilirubin per min/ml under standard assay conditions.

2.3. Preparation of SiO_2@ ZrONPs

SiO_2@ZrONPs were prepared by the precipitation method (Stober et al., 1968). To a mixture of TEOS (2.0 ml) and ethanol (20 ml) in a 50 ml beaker, NH_4OH (4.0 ml) was added dropwise. The mixture was stirred for 8 h and centrifuged at 4000 rpm for 5 min. The white colored silica oxide nanoparticles (SiO_2NP) generated were dispersed into DW (10 ml). ZrONPs (200 μl) suspension was added to this SiO_2NP suspension and its pH was brought to pH 10–10.5, by adding NH_4OH. The zirconia coated silica nanoparticles (SiO_2@ ZrONPs) formed were kept at 40 °C for drying. The characterization of zirconia coated silica nanoparticles was carried out by recording its UV and visible spectra in a UV–visible spectrophotometer, X-ray diffraction pattern in an X-ray diffractometer (XRD) and transmission electron micrograph in a transmission electron microscope.

2.4. Electrodeposition of SiO_2@ZrONPs/CHIT hybrid film onto Au electrode

The surface of Au electrode was polished with alumina slurry (diameter 0.05 μm), followed by washing with DW and sonication in ethanol to remove adsorbed particles and finally washing with DW to remove ethanol. The cleaned electrode was dipped into 25 ml 1 M KCl containing chitosan (0.2%, 200 μl) and SiO_2@ ZrONPs suspension (200 μl) and subjected to 20 successive deposition cycles at −0.1 to 0.2 V using a potentiostat–galvanostat (Fig. 1). The resulting SiO_2@ZrONPs/CHIT modified Au electrode was washed thoroughly with DW to remove unbound matter and kept in a dry Petri-plate at 4 °C.

2.5. Immobilization of BOx onto SiO_2@ZrONPs/CHIT modified Au electrode

SiO_2@ZrONPs/CHIT modified Au electrode was dipped into 1 ml of 2.5% glutaraldehyde in 0.1 M Tris–HCl buffer (pH 8.5), kept at room temperature for 7 h, washed thoroughly with DW, dipped into 1.5 ml of BOx solution (25 U/ml) and kept overnight at room temperature for immobilization. The resulting electrode with immobilized BOx was washed 3–4 times with 0.1 M Tris–HCl buffer (pH 8.5) to remove residual unbound protein. The BOx immobilized onto a SiO_2@ZrONPs/CHIT modified Au electrode retained 83.47% of the initial activity of free enzymes with a conjugation yield of 3.03 mg/cm^2. The resulting BOx/SiO_2@ZrONPs/CHIT/Au electrode was used as working electrode and stored at 4 °C, when not in use. This working electrode was characterized by SEM at different stages of its construction.

2.6. Scanning electron microscopy of enzyme electrode

The SEM images of bare Au electrode and SiO_2@ZrONPs/CHIT/Au electrodes were taken in a scanning electron microscope (Zeiss EV040) at Jawaher Lal Nehru University, New Delhi, on commercial basis.

2.7. Construction and testing of bilirubin biosensor

The enzyme electrode (BOx/SiO_2@ZrONPs/CHIT/Au) as working electrode, Ag/AgCl as reference and Pt wire as counter electrode, were connected through potentiostat/galvanostat. Cyclic voltammogram (CV) of the BOx/SiO_2@ZrONPs/CHIT/Au electrode was recorded

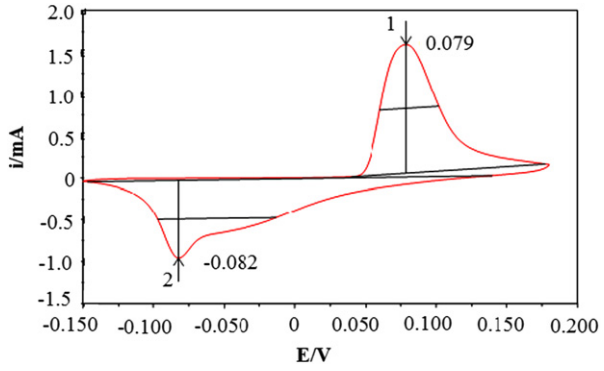

Fig. 1. Cyclic voltammogram for electrodeposition of SiO_2@ZrONPs/CHIT composite film. Supporting electrolyte: 1 M KCl solution; scan rate: 20 mV s^{-1}.

in 25 ml of 0.1 M Tris–HCl buffer (pH 8.5) containing 100 μl of 34.21 μM bilirubin in the potential range −0.05 to 0.5 V vs. Ag/AgCl using a potentiostat–galvanostat.

2.8. Optimization of bilirubin biosensor

To optimize working conditions of the biosensor, effects of pH, incubation temperature, time and substrate (bilirubin) concentration on biosensor response were studied. To determine optimum pH, the pH of reaction buffer was varied from pH 7.0 to 10.0 at an interval of pH 0.5 using the following buffer, each at a final concentration of 0.1 M: pH 7.0–7.5, sodium phosphate buffers and pH 8.0–10.0, Tris–HCl buffer. Similarly to determine optimum temperature, the reaction mixture was incubated at different temperatures (20–50 °C). The effect of substrate concentration on biosensor response was determined by varying the concentration of bilirubin in the range 0.02–250 μM.

2.9. Application of bilirubin biosensor in sera

Blood samples (1 ml each) were drawn from apparently healthy males and females (25 each) and persons suffering from jaundice at Pt. BDS PGIMS, Rohtak hospital and centrifuged at 1500*g* for 10–15 min and their supernatants (sera) were collected. Bilirubin level in sera was determined by the present biosensor in the manner, as described for its response measurement, under its optimal working conditions except that bilirubin was replaced by serum. The bilirubin content in serum was interpolated from standard curve between bilirubin concentration vs. current in milliampere prepared under optimal assay conditions of BOx/SiO_2@ZrONPs/CHIT/Au enzyme electrode (Supplementary Fig. 1)

2.10. Storage stability of BOx/SiO_2@ZrONPs/CHIT/Au electrode

To study the storage stability of the enzyme electrode, its activity was tested weekly for 4 months during its storage at 4 °C in dry condition.

3. Results and discussion

3.1. Characterization of SiO_2@ZrONPs

Fig. 2A shows UV and visible spectra of SiO_2@ZrONPs hybrid film with a strong absorbance peak at 240 nm, confirming the synthesis of SiO_2@ZrONPs. The XRD patterns of the prepared SiO_2@ZrONPs (Fig. 2B) exhibited the characteristic peak of SiO_2@ZrONPs corresponding to the presence of monoclinic phase. No characteristic peaks of impurities were observed, revealing the high purity of SiO_2@ZrONPs. The typical TEM images of SiO_2@ZrONPs nanoparticles (Fig. 2C) showed the spherical shape of SiO_2@ZrONPs nanoparticles with an average size of 20–50 nm.

3.2. Characterization of the enzyme electrode at various stages of its fabrication

3.2.1. By SEM

The SEM images of the surface of bare Au electrode, SiO_2@ZrONPs/CHIT/Au electrode and BOx/SiO_2@ZrONPs/CHIT/Au electrode are shown in Fig. 3A (a), (b) and (c) respectively. The stepwise modification of the electrode could be seen clearly from these SEM images. The SEM image of the bare Au electrode showed a smooth and featureless morphology (Fig. 3a). The SiO_2@ZrONPs/CHIT/Au composite film exhibited a net structure. The film is more uniform and porous (Fig. 3b), hence effective surface area is larger. On immobilization of BOx, the globular structural morphology appeared due to the covalent interaction between SiO_2@ZrONPs/CHIT/Au electrode with BOx (Fig. 3c).

3.2.2. By FTIR spectroscopy

Fig. 3(B) shows FTIR spectra of SiO_2@ZrONPs/CHIT/Au electrode (curve i) and BOx/SiO_2@ZrONPs/CHIT/Au electrode (curve ii). FTIR spectra of electrodeposited SiO_2@ZrONPs/CHIT/Au composite showed bands at 2898 cm^{-1} and 1126 cm^{-1} (curve i) due to the stretching vibration mode of –OH and $-NH_2$ group. The peak at 1762 cm^{-1} is assigned to C–O stretching, while the peak at 1549 cm^{-1} is attributed to amide I group (C–O stretching along with the N–H deformation mode) and 1125 cm^{-1} to the stretching vibration mode of the hydroxyl group as shown in curve ii. This change indicates that the enzyme was attached to the SiO_2@ZrONPs/CHIT/Au composite film. The successful covalent immobilization of BOx onto the SiO_2@ZrONPs/CHIT/Au composite film was indicated by the appearance of the IR absorption of amides I and II.

3.3. Construction of the enzyme electrode

Fig. 4 summarizes the construction of enzyme electrode showing the covalent immobilization of BOx on SiO_2@ZrONPs decorated CHIT film electrodeposited onto the surface of Au electrode. CHIT and SiO_2@ZrONPs were co-electrodeposited on the surface of Au electrode, as this method is easy and the layer thickness could be controlled. To construct the enzyme electrode, BOx was immobilized covalently onto the SiO_2@ZrONPs/CHIT/Au electrode through glutaraldehyde coupling. One −CHO group of glutaraldehyde was bound to $-NH_2$ group of chitosan on the ZrONPs–CHIT composite film, while the other –CHO group gets linked to the free $-NH_2$ group of enzyme surface through C═N bond and thus the enzyme is linked covalently, which provided a physically more stable complex. The CVs of SiO_2@ZrONPs/CHIT/Au exhibited higher currents than CHIT/Au, revealing that the SiO_2@ZrONPs/CHIT/Au composite film have large effective surface area than CHIT/Au composite film and SiO_2@ZrONPs/CHIT/Au composite film could provide a conducting path through the composite matrix for faster kinetics. Hence, the SiO_2@ZrONPs acting as electron transfer mediator help in enhancing the biosensor response and thus increases its sensitivity.

3.4. Cyclic voltammeric (CVs) response measurement of bilirubin biosensor

The maximum response (current in mA) was observed at 0.24 V and hence subsequent studies were carried out at this voltage. Amperometric response of BOx/SiO_2@ZrONPs/CHIT/Au increases by the addition of 100 μl (0.05 mM) bilirubin at the applied potential of 0.24 V (Supplementary Fig. 2). The optimum working potential of present bilirubin biosensor was lower than earlier reported amperometric bilirubin biosensor based on a multilayer network enzyme electrode (0.4 V) (Shoham et al., 1995), nanoporous silicon electrode (0.6 V) (Song et al., 2007), a conductive poly-terthiophene–Mn(II) complex (0.38 V) (Rahmana et al., 2008) and ferrocenecarboxamide modified MWCNT–gold nanocomposite (0.45 V) (Wang et al., 2009). The lowering of the working potential in the present biosensor might be due to the presence of SiO_2@ZrONPs/CHIT/Au, which provides an environment for the enhanced electrocatalytic effect and a fast electron-transfer rate. The SiO_2@ZrONPs and CHIT had a synergistic electrocatalytic effect toward the oxidation of H_2O_2. The synergistic influence of SiO_2@ZrONPs and CHIT contributes to the excellent performance of the biosensor. The existence of SiO_2@ZrONPs and CHIT provides a favorable potential window and electrocatalytic behavior for the H_2O_2 electron transfer to the electrode. The ability of SiO_2@ZrONPs to promote the electron transfer of H_2O_2, suggests

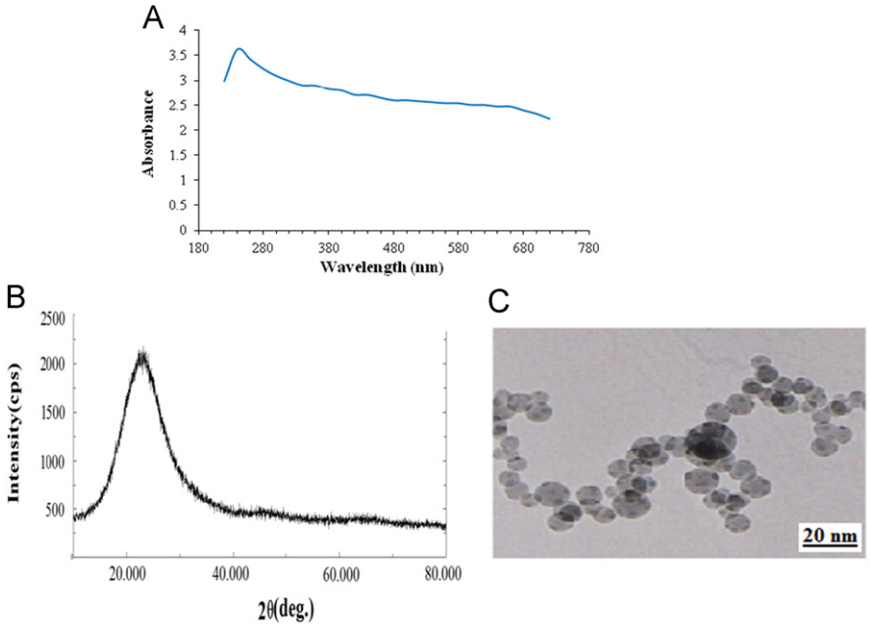

Fig. 2. UV–visible spectra of (A) SiO_2@ZrONPs, (B) X-ray diffraction (XRD) pattern of SiO_2@ZrONPs and (C) transmission electron microscopic (TEM) image of SiO_2@ZrONPs.

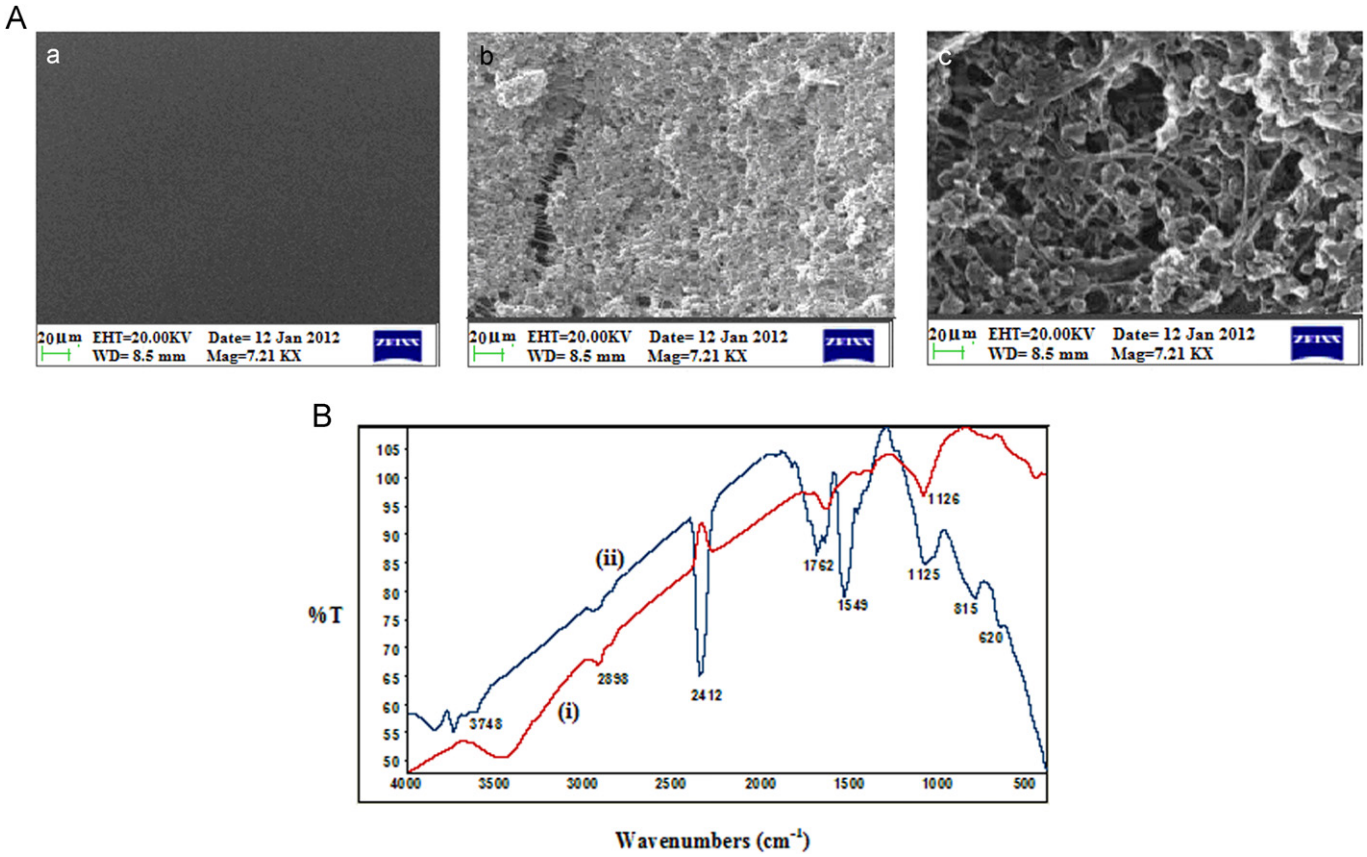

Fig. 3. (A) SEM images of (a) bare Au electrode, (b) SiO_2@ZrONPs/CHIT, and (c) BOx/SiO_2@ZrONPs/CHIT/Au electrode. (B) FTIR spectra of (i) SiO_2@ZrONPs/CHIT, and (ii) BOx/SiO_2@ZrONPs/CHIT/Au electrode.

that SiO_2@ZrONPs have great promise as oxidase based biosensors (Supplementary Table 1). When bilirubin was added into the buffer solution, the oxidation current rose steeply to reach a stable value (Supplementary Fig. 3). The biosensor responded very rapidly, producing 95% of the steady-state current within 2 s (Supplementary Fig. 4). This response time is lower than earlier reported bilirubin biosensors based on a conductive poly-terthiophene–Mn(II) complex (<5 s) (Rahmana et al., 2008) and ferrocenecarboxamide modified MWCNT–gold nanocomposite (less than 5 s) (Wang et al., 2009).

3.5. Electrochemical impedance measurements

Fig. 5 shows electrochemical impedance spectra (EIS) of (i) bare Au electrode (ii) SiO_2@ZrONPs/CHIT/Au electrode and (iii) BOx/

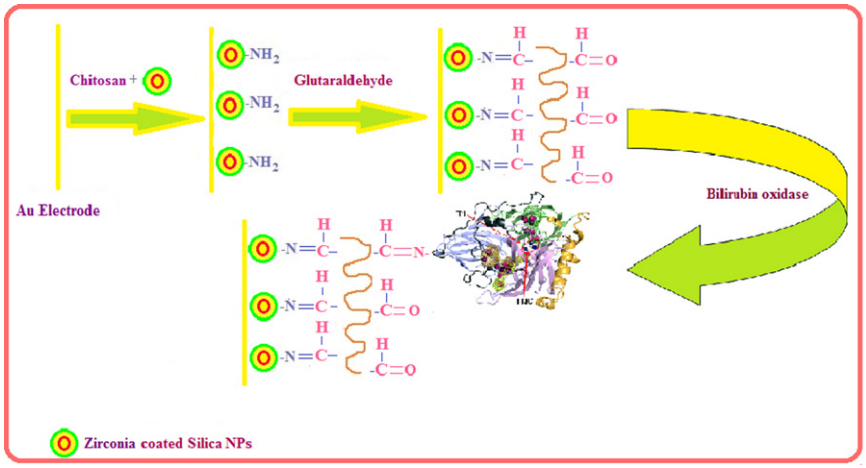

Fig. 4. Schematic representation of the chemical reaction involved in the fabrication of BOx/SiO_2@ZrONPs/CHIT/Au electrode.

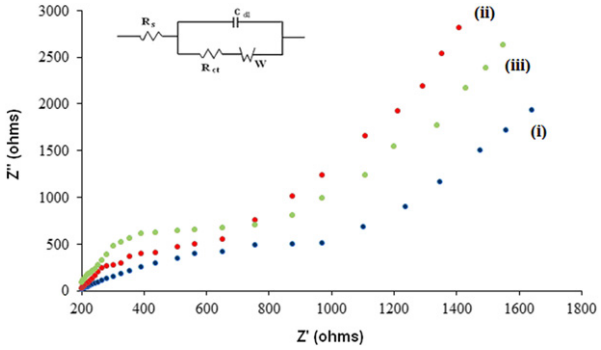

Fig. 5. Impedance spectroscopy study of (i) bare Au, (ii) SiO_2@ZrONPs/CHIT/Au and (iii) BOx/SiO_2@ZrONPs/CHIT/Au in 5 mM $K_3Fe(CN)_6/K_4Fe(CN)_6$ (1:1) as a redox probe.

SiO_2@ZrONPs/CHIT/Au electrode in 5 mM $K_3Fe(CN)_6/K_4Fe(CN)_6$ (1:1) as a redox probe. The diameter of the semicircle portion at higher frequencies of the Nyquist plot was equal to the charge transfer resistance (R_{CT}), which controls the electron transfer kinetics of the redox probe at the electrode interface. The charge transfer process in BOx/SiO_2@ZrONPs/CHIT/Au electrode was studied by monitoring R_{CT} at the electrode and electrolyte interface. The value of the R_{CT} (semicircle diameter) depends on the dielectric and insulating features at the electrode/electrolyte interface. The R_{CT} values for bare Au electrode, SiO_2@ZrONPs/CHIT/Au electrode and BOx/SiO_2@ZrONPs/CHIT/Au electrodes were 970 Ω, 650 Ω and 757 Ω, respectively. The R_{CT} of BOx/SiO_2@ZrONPs/CHIT/Au (iii) bioelectrode was higher compared to that of SiO_2@ZrONPs/CHIT/Au (ii) electrode. This increase in R_{CT} can be attributed to the fact that most biological molecules, including enzymes, are poor electrical conductors at low frequencies and cause hindrance to electron transfer. These results also indicate the binding of enzyme onto the SiO_2@ZrONPs/CHIT/Au composite.

3.6. Optimization of biosensor

The experimental conditions affecting the biosensor response were studied in terms of effect of pH, incubation temperature, time and substrate (bilirubin) concentration. The optimum current was obtained at pH 8.5, which is almost similar to the dissolved oxygen metric bilirubin oxidase electrode (pH 8.5) (Klemm et al., 2000) and glassy carbon electrode modified with ferrocenecarboxamide, gold nanoparticles and multiwalled carbon nanotubes (pH 8.0) (Wang et al., 2009). Optimum pH of the enzyme indicates the types of chemical groups involved at the active center of the enzyme. The pH in the immediate vicinity of the immobilized enzyme may change, but in the present study, pH of immobilized enzyme did not change, due to the biocompatible microenvironment provided by the SiO_2@ZrONPs/CHIT/Au composite. The optimum temperature of the biosensor was 30 °C, after which the activity of biosensor decreased due to thermal denaturation of the enzyme. There was a hyperbolic relationship between biosensor response and bilirubin concentration in the range 0.02–300 μM, which is wider than that reported earlier (Yang and Zhang, 2011) (0.0–80 μM).

3.7. Evaluation of biosensor

There was a linear relationship between the current (in μA) and the bilirubin concentration in the range 0.02–250 μM. The detection limit of the present sensor was 0.1 nM ($S/N=3$), which is lower than that of earlier biosensors based on the modification of molecularly imprinted hydroxyapatite (HAP) film onto a quartz crystal by molecular imprinting and the surface sol–gel technique (0.01 μM) (Yang and Zhang, 2011), due to zirconia coated silica nanoparticles/chitosan (SiO_2@ZrONPs/CHIT) which provided high biocompatibility and fast electron transfer rate between the enzyme and electrode. The average recoveries of bilirubin added to blood serum (at levels of 5 mM and 10 mM) were 95.5% and 97.0% demonstrating the satisfactory reliability of the present biosensor (Supplementary Table 2). Within-sample and between-sample coefficients of variation for the determination of bilirubin in serum on the same day and after 1 week of storage were 3.2% and 3.35%, respectively (Supplementary Table 3). These high precisions revealed good reproducibility and consistency of the present method, which can be attributed to the covalent immobilization of bilirubin oxidase onto the SiO_2@ZrONPs/CHIT/Au electrode.

3.8. Application of bilirubin biosensor

The bilirubin level in apparently healthy persons and jaundice patients, as measured by the present biosensor was in the range 01–16 and 21–62 μM, respectively (Supplementary Table 4). In order to determine the accuracy of the present method, bilirubin values in 25 serum samples were determined by the present enzyme electrode method (y) and compared with those obtained by the colorimetric method (x), the values obtained by both the methods were co-related using regression equation. The regression plot between the two methods were drawn and the correlation coefficient was determined by using the following formula with a good correlation ($r=0.99$) (Fig. 6A).

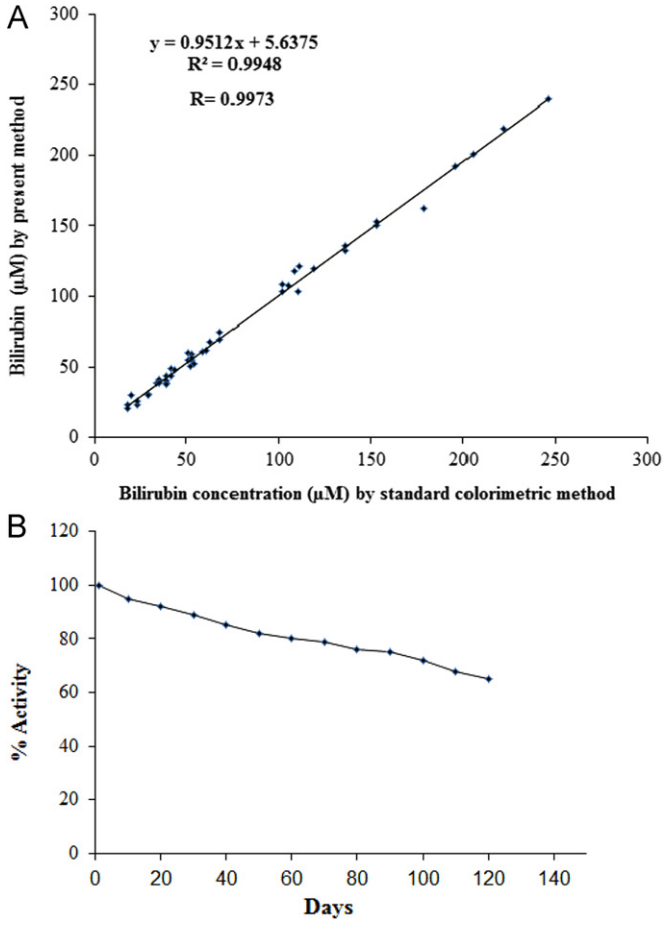

Fig. 6. (A) Correlation between serum bilirubin values measured by the chemical photochlorometric method (x-axis) and the current method (y axis) employing the bilirubin biosensor based on SiO_2@ZrONPs/CHIT/Au composite film, and (B) effect of storage at 4 °C on the response of Box/SiO_2@ZrONPs/CHIT/Au electrodes.

Correlation coefficient (r)

$$r = \frac{n\Sigma xy - \Sigma x \Sigma y}{\{n\Sigma x^2 - (\Sigma x^2)\}\{n\Sigma x^2 - (\Sigma y^2)\}}$$

where x are the values obtained by the standard colorimetric method (Bergmeyer et al., 1985)and y are thevalues obtained by the present enzyme electrode method.

3.9. Interference study and selectivity

The effect of addition of some possible interferents such as uric acid, ascorbic acid, glycine, glucose, uric acid and creatinine on the current response of the present biosensor was studied at their physiological concentrations using 100 μM bilirubin in 0.1 M Tris–HCl (pH 8.5) as reaction mixture. The results showed that none had practically any interference. At comparatively lower working potential (0.24 V), a number of serum substances are unable to undergo electro oxidation and thus do not interfere in the biosensor response.

3.10. Long-term stability of enzyme electrode

The long-term stability of the enzyme electrode was investigated by measuring current response of the biosensor every week under its storage at 4 °C. The enzyme electrode lost only 30% of its initial activity after 150 regular uses over a period of 120 days (Fig. 6B). These observations indicate the better stability of enzyme electrode than earlier enzyme electrodes (Yang and Zhang, 2011) due to the covalent coupling of the enzyme.

4. Conclusion

An improved amperometric bilirubin biosensor was constructed by immobilizing covalently a bilirubin oxidase onto SiO_2@ZrONPs hybrid attached onto Au electrode through chitosan film, which resulted in a relatively rapid response (2 s), broad linear range (0.02–250 μM), low detection limit (0.1 nM), good reproducibility and long stability (4 months at 4 °C).

Appendix A. Supporting information

Supplementary data associated with this article can be found in the online version at http://dx.doi.org/10.1016/j.bios.2012.12.034.

References

Baranano, D.E., Rao, M, Ferris, C.D., Snyder, S.H., 2002. Proceedings of the National Academy of Sciences United States of America 99, 16093–16098.
Bergmeyer, H.U., Horder, M., Rej, R., 1985. Journal of Clinical Chemistry and Biochemistry 24, 481–489.
Doumas, B.T., Perry, B.W., Sasse, E.A., Straumfjord, J.V., 1973. Clinical Chemistry 19, 984–993.
Fortuney, A., Guilbault, G., 1996. Electroanalysis 8, 229–232.
Klemm, J., Prodromidis, M., Karayannis, M., 2000. Electroanalysis 12, 292–295.
Koch, T.R., Oakingbe, O., 1981. Clinical Chemistry 27, 1295–1299.
Li, X.P., Rosenzweig, Z., 1997. Analytica Chimica Acta 353, 263–273.
Liu, Y., Li, P., Lu, J., Xiong, W., Oger, J., Tetzlaff, W., Cynader, M., 2008. Journal of Immunology 181, 1887–1897.
Maisels, M.J., 2009. Early Human Development 85, 727–732.
Rahmana, M., Lee, A.K.S., Park, D.S., Won, M.S., Shima, Y.B., 2008. Biosensors and Bioelectronics 23, 857–864.
Satypal, Pundir, C.S., 1993. Biochimica Biophysica Acta 11, 611–615.
Shoham, B., Migron, Y., Riklin, A., Willner, I., Tartakovsky, B., 1995. Biosensors and Bioelectronics 10, 341–352.
Song, M.J., Yun, D.H., Min, N.K., Hong, S.I., 2007. Journal of Bioscience and Bioengineering 103, 32–37.
Stober, W., Fink, A., Bohn, E.J., 1968. Journal of Colloid and Interface Science 26, 62–69.
Wang, C., Wang, G., Fang, B., 2009. Microchimica Acta 164, 113–118.
Wang, J., Lou, D.B., Farias, P.A.M., 1985. Journal of Electroanalytical Chemistry 185, 61–71.
Wang, J., Ozsoz, M., 1990. Electroanalysis 2, 647–650.
Wang, Y., Zhang, X., Chen, Y., Xu, H., Tan, Y., Wang, Shengfu, 2010. American Journal of Biomedical Sciences 2, 209–216.
Yang, Z., Zhang, C., 2011. Biosensors and Bioelectronics 29, 167–171.